CAVITATION EROSION MECHANISM: NUMERICAL SIMULATIONS OF THE INTERACTION BETWEEN PRESSURE WAVES AND SOLID BOUNDARIES

R. FORTES-PATELLA, G. CHALLIER, JL. REBOUD(*)
Laboratoire des Ecoulements Géophysiques et Industriels, Grenoble, France
(*) Ecole Nationale d'Ingénieurs de Saint Etienne/LTDS

A. ARCHER
Electricité de France EDF – R&D Division, Chatou, France

Abstract
To evaluate the aggressiveness power of cavitating flows and to improve prediction methods for cavitation erosion, the pressure waves emitted during bubble collapses were studied and simulated by means of the Keller's and Fujikawa and Akamatsu's physical models. The profile and the energy of the pressure waves emitted during cavity collapse were evaluated by numerical simulation. The dynamic response and the surface deformation (i.e., pit profile and pit volume) of various materials exposed to pressure wave impacts was simulated making use of a 2D axisymmetric numerical code simulating the interaction between pressure wave and an elastoplastic solid. Making use of numerical results, a new parameter β (defined as the ratio between the pressure wave energy and the generated pit volume) was introduced and evaluated for three materials (aluminum, copper and stainless steel). By associating numerical simulations and experimental results concerning pitted samples exposed to cavitating flows (volume damage rate), the pressure wave power density was introduced. This physical property of the flow characterizes the cavitation aggressiveness and can be related to the flow hydrodynamic conditions. Associated to β parameter, the pressure wave power density appeared to be a useful tool to predict the cavitation erosion power.

NOMENCLATURE

Liquid / Pressure wave emission:

C_∞	: celerity of pressure wave	(m/s)
δt	: wave passage time	(s)
E_{wave}	: pressure wave energy	(J)
L	: distance emission center - solid boundary	(m)
P	: peak pressure applied on solid surface	(N/m^2)
Pmax	: peak of the transient pressure signal	(N/m^2)
P_∞	: initial fluid pressure	(N/m^2)
p	: static pressure	(N/m^2)
r	: radial distance from wave emission center	(m)
v	: mean flow velocity	(m/s)
ρ	: fluid density	(kg/m^3)
ρ_∞	: initial fluid density	(kg/m^3)
σ_c	: cavitation number	

$$\sigma_c = (P_{downstream}-P_{vapor})/P_{upstream}$$

• dots denote differentiation with respect to time

Solid :

C_L	: celerity of longitudinal waves	(m/s)
E	: Young's modulus	(N/m^2)
H	: pit depth	(m)
$R_{10\%}$	: pit radius at 10% of H	(m)
S_0	: yield limit for simple shear stress	(N/m^2)
V_{pit}	: pit volume	(m^3)
$\beta_{material}$	: mechanical characteristic coefficient	(J/mm^3)
ν	: Poisson's ratio	

Pitted Samples :

$P_{wave}/\Delta S$	: pressure wave power density	(W/m^2)
V_d	: volume damage rate	($\mu m^3/mm^2/s$
V_d *	: corrected volume damage rate	($\mu m^3/mm^2/s$)
ΔS	: analyzed sample surface	(m^2)
ΔT	: test duration	(s)

• the term pit is used to refer to the plastic deformation observed on material surface

1. Introduction
Many works have been developed last years in order to gain better knowledge concerning cavitation erosion mechanism [1-6]. In the industrial point of view concerning both machine design and maintenance, the evaluation of the erosion power of cavitating flows and the prediction of the material damage remains a major concern for machinery manufacturers and users.

According to previous works [4,7], pressure waves emitted during the collapses of vapor structures seem to be the main factor contributing to cavitation damage. The emission of the pressure waves can be generated either by spherical bubble or vortex collapses (as observed by [8] and [9]) as well as by micro jet formation [10]. The emitted pressure waves interact with neighboring solid surfaces, leading to material damage. Previous work [7] indicated that the damage of material due to cavitation phenomena could be related to the characteristics (mainly the energy) of the pressure wave emitted by vapor structures collapses.

In this context, the present work aims to simulate and to analyze the emission of pressure waves during bubble collapses and their interaction with neighboring solid surfaces.

The first part of the paper (section 2) presents a theoretical and numerical analysis of pressure waves emitted during spherical bubble collapses. The Keller's model [11] is applied to simulate numerically the dynamic behavior of cavitation bubbles in water. The characteristics of the pressure wave emitted during the bubble implosion (such as signal shape, wave passage time, wave amplitude and emitted energy) were calculated as a function of hydrodynamic conditions (i.e., surrounding pressure, air contents and bubble radius) [12].
The second part of the paper (section 3) concerns the material damage due to the pressure wave impact. By associating the proposed pressure wave model with an elastoplastic solid code developed by [13], it was possible to build a 2D axisymmetric coupled fluid-structure model to study the interaction between the pressure wave and the material surface. The section 3 presents numerical results obtained concerning mainly the permanent surface deformation of the solid surface and the energy balance between pressure wave phenomenon and material damage. The proposed energetical approach is applied in the case of different hydrodynamic conditions (i.e., pressure wave characteristics) and solid properties (aluminum, copper, stainless steel).
The main application of our study, presented in section 4, is related to the evaluation of cavitation aggressiveness. Based on the Knapp's approach [14], which proposed to use the material as a sensor to evaluate the cavitation erosion power, we analyzed pitted samples exposed to cavitating flows. A methodology to evaluate and to correct the volume damage rates obtained by pitting analysis is also introduced to rectify the influence of test duration and of the cut-off parameters [15].
Making use of results obtained by numerical simulation and by analyzing pitted samples, the pressure wave power density, which represents the flow cavitation aggressiveness, is defined and calculated for different flow velocities.

2. Pressure wave simulation

a) Bubble collapse model

To simulate the spherical bubble collapses, we have applied the model proposed by [11], based on the Kellers's approach [16]. In this model, the following hypothesis are taken into account: the vapor/gas bubble is and remains spherical, the fluid is infinite, compressible and viscous; the pressure within the bubble is uniform; the non-condensable gas inside the bubble is inviscid and obeys the perfect-gas adiabatic law; the physical properties of liquid and gas are constant; heat conduction and thermal effects are not taken into account; the interaction between compressibility and viscosity, and the effect of gravity and gas diffusion are negligible.
The equation of the motion, describing the bubble dynamic, is:

$$\left[1-\frac{\dot{R}}{C_\infty}\right]R\ddot{R}+\frac{3}{2}\left[1-\frac{1}{3}\frac{\dot{R}}{C_\infty}\right]\dot{R}^2=\left[1+\frac{\dot{R}}{C_\infty}+\frac{R}{C_\infty}\frac{d}{dt}\right]\frac{P_B}{\rho}$$

$$\text{with } P_B=p_v+P_g-P_\infty(t)-\frac{2s}{R}-\frac{4m}{R}\dot{R}$$

where R is the bubble radius; C_∞ is the sound speed in the liquid (assumed constant according to the acoustical approximation); p_v and P_g are the vapor pressure and the gas pressure inside the bubble; μ is the liquid viscosity; σ is the surface tension; ρ is the liquid density and P_∞ is the pressure at infinity. The gas pressure inside the bubble is calculated considering adiabatic conditions:

$$P_g=P_{g0}\left(\frac{R_0}{R}\right)^{3g}$$

where P_{g0} and R_0 are respectively the initial gas pressure and bubble radius, and γ is the ratio of the specific heats (γ =1.4 for air).

b) Pressure signal

To simulate the time and spatial pressure distribution throughout the liquid during bubble collapse, the study considers:

- the Tait state equation given by [17]:

$$\frac{P+B}{P_\infty+B}=\left(\frac{r}{r_\infty}\right)^n$$

where P is the liquid pressure, P_∞ the pressure at infinity, ρ the liquid density and ρ_∞ the density at infinity. B is 3010 atm and the index n is 7.15 for water.

- the Fujikawa and Akamatsu,'s model [18], which uses a first-order approximation of the velocity potential $\phi(r,t)$ for the liquid. The time and spatial pressure distribution in the liquid can be then calculated by the equation:

$$p(r,t) = -B + (p_\infty + B)\left[1 - \frac{n-1}{c_\infty^2}\left(\frac{\partial \Phi}{\partial t} + \frac{1}{2}\left(\frac{\partial \Phi}{\partial r}\right)^2\right)\right]^{\frac{n}{n-1}} \qquad f = -\frac{1}{r}\left[R^2\dot{R} - \frac{R^2}{c_\infty}\left(2\dot{R}^2 + R\ddot{R}\right)\right]$$

In the present work, the differential equations were numerically integrated by the 4th order Runge-Kutta method. In order to validate the numerical code, we compared results obtained with ones available in the literature [18-19]. Results were presented in [12].

Several simulations have been performed to study the pressure waves emitted during the bubble collapse. According to the numerical study, the emitted pressure signals can be represented by a non-dimensional distribution, as indicated by the Figure 1. Pressure waves are characterized by the maximum amplitude Pmax at a given radial distance "r" from the wave emission center, and by the wave passage time δt (given by the pressure signal width at p=Pmax/2).

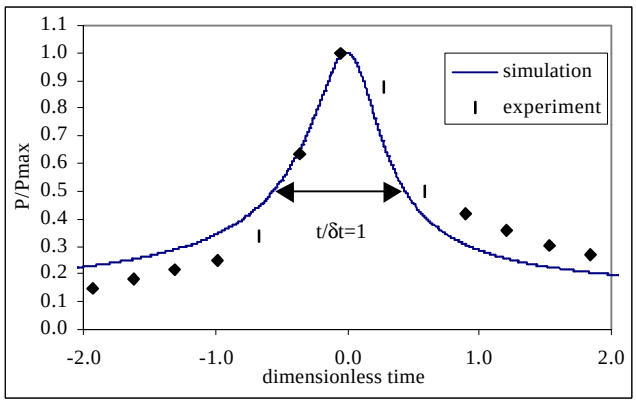

Figure 1: Non dimensional pressure signal obtained by numerical calculations and experiments [19]. Dimensionless time is defined as t/δt.

Figure 1 illustrates also the comparison between the numerical and experimental results concerning the non-dimensional shape of the pressure wave. Experimental work has been developed by [19] in the Laboratory LP3 of Marseille. The collapses of single bubbles generated by a laser pulse have been studied and the pressure signal emitted during bubble collapse was measured by a PVDF transducer, placed at 8.6 mm away from the center of the bubble. We have observed a good agreement between experiments and numerical results concerning the pressure wave non-dimensional shape and pressure amplitudes. This study was detailed in [20].

c) Pressure wave energy

Pressure waves created by bubble collapses are also characterized by the emitted energy E_{wave}, which can be evaluated by the acoustic energy approach [7-9]:

$$E_{wave} = \frac{4\pi r^2}{\rho C_\infty}\int p^2 dt \approx \frac{4\varsigma\pi P_{max}^2 r^2}{\rho C_\infty}\delta t$$

where p is the transient pressure signal at a given radius "r", Pmax is the peak of the pressure signal at radius “r”, C_∞ is the pressure wave celerity, ρ is the fluid density, and δt is the wave passage time.

The factor ζ is related to the waveform of the pressure signal (for signal illustrated by Figure 1, ζ is equal to 1). This method was also used by [21] to determine the acoustic energy spectrum and the noise level due to bubble collapses.

3. Pressure wave/material coupling

To study the local aspects of cavitation erosion we performed a pressure wave-solid coupling code, which simulates the plastic deformation of materials subjected to the impact of spherical pressure wave emitted to a distance "L" to the solid surface during the bubble collapses [4].

a) Solid code

The material’s response to the pressure wave impact is calculated by a finite-element numerical code (SOLID Model), which involves a Lagrangian formulation in cylindrical co-ordinates [13]. It takes into account the laws of continuum mechanics (mass conservation and the fundamental law of the dynamics) and an elastoplastic constitutive equation. The material’s behavior is described by four independent factors: Young's modulus E, Poisson's ratio ν, celerity of the

longitudinal wave C_L (involving E, ν and the material density), and a yield limit for the simple shear stress S_0. The code provides the complete transient evolution of strain, stress and energy fields within the material and mainly the permanent surface deformation resulting from pressure wave impact. One notes that the code does not take into account the mass loss, and it can describe only the incubation stage of cavitation erosion.
The code considers symmetry conditions along the axis of revolution. The pressure spatial and temporal signal presented here above in the case of pressure waves emitted during bubble collapses are used by the SOLID code as the boundary conditions at the wetted surface of the material, as illustrated by Figure 2.
Moreover, the other solid boundaries are considered to be non-reflecting with respect to the longitudinal and transversal stress waves.

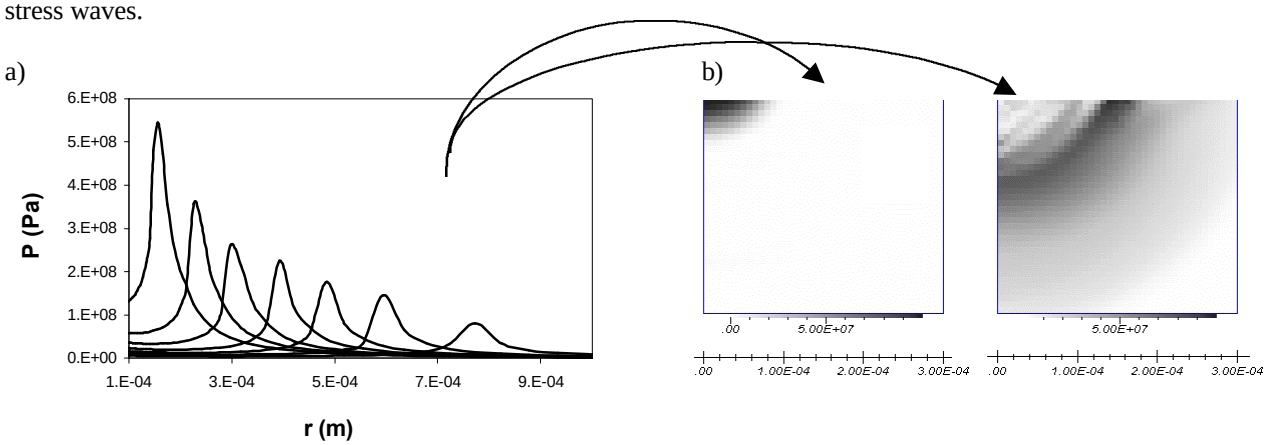

Figure 2: a) spatial pressure signal applied to the solid surface at seven different times. b) stress field (second invariant of the deviatoric part) in the material due to the pressure wave impact at two different times. Results are given in N/m^2. The co-ordinates are cylindrical axisymmetric and only one meridian half-plane is presented

b) Material damage

According to numerical simulations concerning different materials submitted to pressure wave impacts [4], the material damage can be represented by a non-dimensional axisymmetric indentation, as illustrated in Figure 3. The figure shows a good agreement between numerical non-dimensional pit profile and experimental ones observed on samples of different materials exposed to several cavitation conditions.

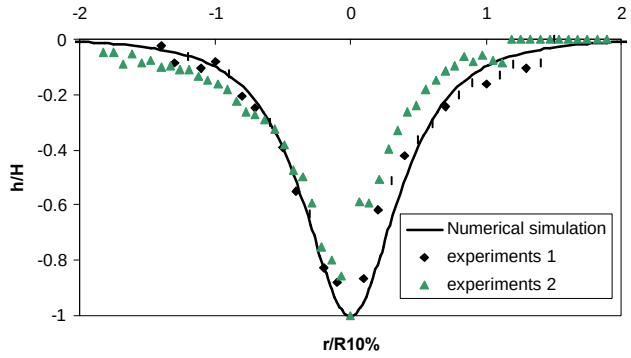

Figure 3: Permanent surface deformation (non dimensional pit profile) calculated for pressure wave impact on material surface. Numerical results are compared with experimental ones obtained by 3D laser profilometry under different cavitation conditions. Pit profile is characterized by the radius $R_{10\%}$, depth H and volume V_{pit} obtained by trapeze integration. The damage is characterized by a plastic deformation of the surface material, without mass loss.

c) Energetical approach

To improve our previous works concerning the energy balance between pressure wave energy and material damage [7], many numerical simulations have been done by considering different material properties and wave amplitudes. Three materials have been analyzed: aluminum, copper and stainless steel. Table 1 gives the mechanical characteristics used by the simulations.

According to the simulations, the solid damage represented by the pit volume V_{pit} seems to be directly proportional to the pressure wave energy as indicated by Figure 4:

$$E_{wave}=\beta V_{pit}$$

We observe that the parameter β depends strongly on the solid properties but it is almost independent on the impact amplitude. It is worth noting that, for smaller impact energy, the elastic behavior of materials becomes more relevant, leading to some numerical instabilities concerning mainly solid deformation calculations.
Figure 4 illustrates numerical results concerning the evaluation of the β parameter for the three materials:

$\beta_{aluminum}$~4 (±0.4) J/mm^3, β_{copper}~20 (±3) J/mm^3 and $\beta_{stainless\ steel}$~30 (±2) J/mm^3 [(1)].

	S_0 (MPa)	E (GPa)	C_L (m/s)	n
Aluminum	100	50	5000	0.30
Copper	200	120	4700	0.33
S. Steel	200	200	5800	0.30

Table 1: Material mechanical properties applied by numerical code. Calculations concerning stainless steel take into account the material strain hardening.

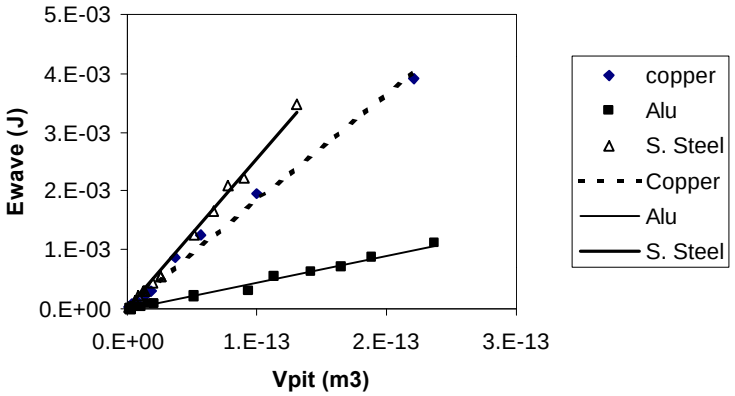

Figure 4: The figure illustrates the relation between the pressure wave energy and pit volume obtained by numerical simulations concerning three materials. Range of the pressure wave characteristics adopted by simulations: 0.8 GPa ≤ P ≤ 4 GPa ; 10 ns ≤ δt ≤ 150 ns ; 10 μm ≤ L ≤ 100 μm.

Indeed, the value of the coefficient β is strongly related to the characteristic of the materials, mainly to the value of the yield limit for simple shear stress S_0. In order to evaluate the influence of this parameter on the evaluation of β, many simulations have been performed considering stainless steel properties (E, ν and C_L) for a range of 100MPa≤S_0≤450MPa. Results are illustrated by Figure 5. We can note that the β value increases when S_0 rises, according to a power law. The same behavior was observed in the case of aluminum and copper simulations.
It is worth noting that the numerical code uses material static properties. To improve quantitative analysis, more information is needed concerning the mechanical behavior of materials at very high strain rates and their dynamic properties.

4. The material used as a sensor

Based on the results presented here above concerning the energy balance between pressure wave and material damage, the aim of this section is to evaluate cavitation aggressiveness by analyzing pitted sample exposed to cavitating flows.

a) Experimental study

This study involved analyzing experimental results obtained by Electricité de France [22] in MODULAB Test Rig. Samples in several materials were damaged by water cavitating flow downstream a diaphragm, which generates jet cavitation (Figure 6). Tests were performed for a constant cavitation number σ_c=0.7 and different water flow velocities (Table 2a). Water is demineralized and deaerated. The air content is controlled with an oxygenmeter and the oxygen rate is maintained less than 3 ppm.

[1] Standard deviations are presented in parenthesis.

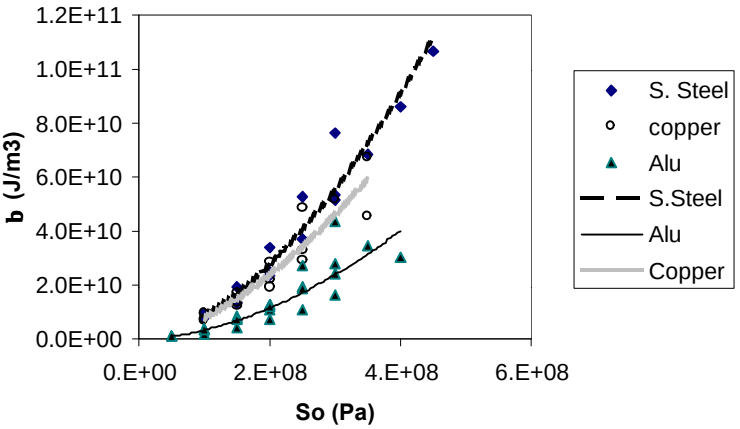

Figure 5: Evaluation of β parameter as a function of the stress limit S_0.

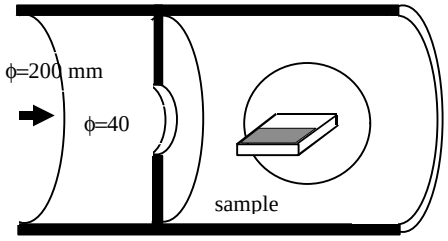

Figure 6: MODULAB test rig. The cavitation appears in the wake zone of the jet. Generated vapor structures are convected downstream, and the samples are damaged during the collapses of these vapor structures.

b) Pitted sample analysis

The erosion of the sample surfaces was measured by a UBM16 laser profilometer device. According to the manufacturer, the accuracy for depth measurements is 0.06 µm. Pit radius measurements are made with 1 µm lateral resolution.

Special software was developed to scan the surface of the pitted samples [15]. This code gives the location and size (depth « H », radius « $R_{10\%}$ » and volume « V ») of each individual pit. It supplies also the volume damage rate « Vd » (i.e., the ratio between deformed volume, analyzed sample surface and test duration) for each analyzed sample.

Generally, one assumes a linear behavior between total volume damage ΣV and test duration ΔT (i.e., Vd would be constant for different test durations). Indeed, experimental study [15] seems to indicate dependence between Vd and ΔT for a sample surface ΔS constant. This phenomenon could be explained by the existence of superposed impacts, whose number increases with test duration ΔT.

In order to perform an adequate evaluation of the volume damage rate, the measured value of Vd should be corrected to eliminate the influence of the test duration and of the analysis cut-off parameter (related to the measurement resolution threshold). Table 2b presents the values of the volume damage rate before (Vd) and after (Vd*) correction. Vd* represents the volume damage rate corresponding to a small reference time t*=1/f characteristic of the considered cavitation condition (flow velocity v, cloud shedding frequency f, …). The methods applied to evaluate Vd* are detailed in [15] and [23].

c) Pressure wave power density

To analyze samples exposed to different flow hydrodynamic conditions, the pressure wave power density P_{wave}/DS obtained from experimental results is introduced:

$$\frac{P_{wave}}{\Delta S} = \frac{(\Sigma E_{wave})}{\Delta T \Delta S} = \beta \frac{(\Sigma V_{pit})}{\Delta T \Delta S} = \beta V_d^*$$

where ΔS is the analyzed sample surface (10 x 10 mm^2), and ΔT is the test duration (s). (ΣEwave) represents the total relevant wave energy detected by the sample surface during cavitating tests.

Results concerning the evaluation of the pressure wave power density are illustrated by Figure 7. It appears that for a same cavitating flow, the wave power density is constant, independently on the sample materials:

$$\frac{P_{wave}}{\Delta S} = \left(\beta Vd^{*}\right)_{aluminum} = \left(\beta Vd^{*}\right)_{copper} = \left(\beta Vd^{*}\right)_{stainless\ steel}$$

Thus, the pressure wave power density seems to well represent the cavitation aggressiveness of the flow and can be related to the flow hydrodynamic characteristics: it increases approximately as $P_{wave}/DS \sim v^5$ as illustrated by Figure 7.

v (m/s)	DT (s)	Vd ($mm^3/mm^2/s$)	Vd* ($mm^3/mm^2/s$)
20	Aluminum: 120 Copper: 300 S. Steel: 7200	871 95.5 3.5	1023 140 69
25	Aluminum: 60 Copper: 120 S. Steel: 3600	2640 414 8.5	3087 560 161
32	Aluminum: 30 Copper: 60 S. Steel: 1800	9030 1110 28	10603 1513 553
38.5	Aluminum: 21 Copper: 30 S. Steel: 900	19700 3840 59	23912 5042 1006

a) Tests conditions b) Volume damage rate

Table 2: Experimental tests realized in MODULAB for aluminum, copper and stainless steel samples ($\Delta S=100mm^2$).

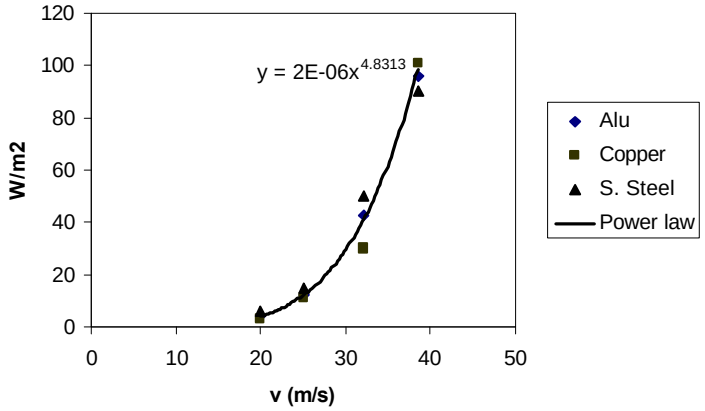

Figure 7: Pressure wave power density (measured by three different materials) as a function of the flow velocity. For tested stainless steel samples, $S_0 \approx 400$ MPa and $\beta \approx 90$ J/mm^3.

5. Conclusion

The interaction between pressure wave emitted during vapor structures collapses and neighboring solid boundaries was analyzed by means of numerical calculations concerning spherical bubble implosions and material deformation.

Pressure wave signals obtained by simulations appeared to be well represented by a universal non-dimensional distribution relating maximum pressure amplitude, wave energy and passage time.

The permanent surface deformation calculated for pressure wave impact on material surface seemed to be also well characterized by a non dimensional pit profile.

According to the simulations, material damage (represented by pit volume) is directly related to the pressure wave energy via the mechanical coefficient β, characteristic of solid behavior.

The analysis of pitted sampled exposed to cavitating flows associated with numerical calculations leaded to the evaluation of the pressure wave power density, characteristic of flow aggressiveness. Results indicated that the evaluation of the pressure wave power density and the mechanical coefficient β are a useful tool in the prediction of cavitation erosion concerning:

- the influence of solid properties on material damage
- and the effect of flow velocity on cavitating flow aggressiveness.

Further works, requiring more experimental data, are in progress to:
- validate the proposed methodology to correct volume damage rate obtained by pitting analysis by rectifying the influence of test duration
- evaluate mechanical behavior of materials at high strain rates and their dynamic properties
- improve analysis concerning energy transfer between vapor structure, pressure wave emission and material damage
- predict pressure wave power density from unsteady, two-phase, viscous numerical simulations of cavitating flows [24].

Acknowledgements

This study is supported by EDF-Electricité de France (R&D Division) and by a doctoral grant from the Education French Ministry MERT.

References

[1] Franc, J.P., Michel, J.M., Nguyen-Trong, H., and Karimi, A., 1994, "From Pressure Pulses Measurements to Mass Loss Prediction: The Analysis of a Method", *Proc. 2nd Int. Symp. on Cavitation*, Tokyo, pp. 231-236.

[2] Lecoffre, Y., 1995, "Cavitation Erosion, Hydrodynamics Scaling Laws, Practical Method of Long Term Damage Prediction", *Proceedings of. Int. Symp. on Cavitation, CAV'95,* Deauville, pp. 249-256.

[3] Kato, H., Konno, A., Maeda, M., and Yamaguchi, H., 1996, "Possibility of Quantitative Prediction of Cavitation Erosion Without Model Test", *Journal of Fluid Engineering* , Transactions of the ASME, Vol. 118, pp. 582-588.

[4] Fortes-Patella, R., and Reboud, JL., 1998, "A New Approach to Evaluate the Cavitation Erosion Power", *Journal of Fluid Engineering* , Transactions of the ASME, Vol. 120, June 1998.

[5] Pereira , F., Avellan, F., and Dupont, J.M., 1998, "Prediction of Cavitation Erosion: an Energy Approach", *Journal of Fluid Engineering* , Transactions of the ASME, Vol. 120, December 1998

[6] Boehm, R., Hofmann, M., Ludwig, G., Stoffel, B., 1998, "Investigations on Possibilities to Control de Erosive Cavitation Aggressiveness by Hydrodynamic Effects", *Proc. of 3rd International Symp. on Cavitation*, Grenoble.

[7] Fortes-Patella, R., and Reboud, JL.,1998, "Energetical Approach and Impact Efficiency in Cavitation Erosion", *Proc. of 3rd International Symp. on Cavitation*, Grenoble.

[8] Vogel, A., Lauterborn, W., Timm, R., 1989, "Optical and Acoustic Investigations of the Dynamics of Laser-Produced Cavitation Bubbles Near a Solid Boundary ", *Journal of Fluid Mechanics*, Vol. 206, pp. 299-338.

[9] Ward and Emmony, 1990, "The Energies and Pressures of Acoustics Transients associated with Optical Cavitation in Water", *Journal of Modern Optics*, vol.37, number 4.

[10] Philipp, A., Ohl, C. D., and Lauterborn, W., 1995, "Single Bubble Erosion on a Solid Surface", *Proceedings of Int. Symp. on Cavitation*-CAV'95, Deauville, pp. 297-303.

[11] Prosperetti and Lezzi, 1986, "Bubble Dynamics in a Compressible Liquid. Part I: First Order Theory", *Journal of Fluid Mechanics*, vol 168, pp 457-478.

[12] Fortes-Patella, R., Challier, G., and Reboud, JL., 1999, "Study of Pressure Wave Emitted During Spherical Bubble Collapse", *Proc. of the 3rd ASME/JSME Fluids Eng. Conference*, July, 1999, San Francisco, California.

[13] Reboud, J.L., and Guelin, P., 1988, "Impact Response of an Elasto-plastic Medium", *Mech. Research Communications*, Vol 4.

[14] Knapp, R.T., 1955, "Recent Investigations of the Mechanics of Cavitation and Cavitation Damage", *Trans. ASME*, 75, N° 8, pp. 1045-1054.

[15] Fortes Patella, R., Reboud, JL., and Archer, A., 2000, "Cavitation Mark Measurements by 3D Laser Profilometry", *Journal of WEAR*, vol 246, pp. 59-67.

[16] Keller and Kolodner, 1956, "Damping of Underwater Explosion Bubble Oscillation", *Journal of Applied Physics*, vol 27, number 10 pp 1152-1161.

[17] Cole, 1948, "Underwater Explosions", Dover Publications, New York.

[18] Fujikawa, S., and Akamatsu, T., 1980, "Effects of Non-Equilibrium Condensation of Vapor on the Pressure Wave Produced by Collapse of a Bubble in Liquid", *Journal of Fluid Mechanics*, Vol. 97-3, pp.481-512.

[19] Isselin JC, Alloncle P.and Autric M, 1998, "Investigations of Material Damages Induced by an Isolated Vapor Bubble Created by Pulsed Laser", *Proc. of Third International Symposium on Cavitation*, Grenoble.

[20] Challier, G., Fortes Patella, R., and Reboud, JL., 2000, "Interaction Between Pressure Waves and Spherical Cavitation Bubbles : Discussions about cavitation erosion mechanism", *Proceedings of the 2000 ASME Fluids Engineering Summer Conference*, June 11-15, 2000, Boston, Massachusetts.

[21] Lovik A., and Vassenden J., 1977, "Basic and Applied Aspects of Scaling Cavitation Noise", Conference on Scaling for Performance Prediction in Rotordynamic Machines, University of Stirling, September 1977.

[22] Simoneau, R., and Archer, A., 1997, "Transposition of Cavitation Marks on Different Hardness Metals", *Proceedings of ASME Fluids Engineering Division Summer Meeting*, Vancouver, June 1997.

[23] Challier,G. and Fortes Patella, R., 2001, "Prévision de l'Erosion de Cavitation : Couplage Ecoulement et Matériau", Internal Report, Contract LEGI/EDF N° P41/C03332, April 2001.

[24] Reboud J.L., Stutz B. and Coutier O., 1998, "Two-phase flow structure of cavitation : experiment and modelling of unsteady effects", *Proc. of Third International Symposium on Cavitation*, Grenoble.